# Experimental Analysis of a Time-Dependent FSO System under Summer Conditions in South Korea

Tae-In Oh, Jong-Min Kim, Min-Ji Lee, Young-Chai Ko
School of Electrical Engineering, Korea University, Seoul, Korea
<logan10, botboy0441, ddi06048, koyc>@korea.ac.kr

***Abstract*—In this study, the time-dependent performance of free-space optical (FSO) communication is investigated through a practical experiment. Employing an experimental setup spanning 400 m in an outdoor environment, we measure bit error rate (BER) utilizing BERT (bit error rate tester) automatically, while recording corresponding weather conditions. The experimental results demonstrate that BER performance shows better performance during period without sunlight, indicating a critical role of sunlight. Moreover, the impact of temperature and rainfall on FSO performance is observed. Our practical approach, conducted outdoors and using automated equipment, contribute to a deeper understanding of FSO communication under diverse weather conditions.**

***Index Terms*—Free-space optics (FSO), turbulence, bit-error rate (BER)**

## I. Introduction

Free-space optical (FSO) communication is wireless optical communication in which an optical signal is transmitted through free-space instead of optical fiber. FSO has a variety of benefits such as using unlicensed bands, large bandwidth, low implementation cost, and security [1]. However, the performance of the FSO system is dependent on atmospheric conditions, which results in scattering and attenuation [2]. Due to the unpredictable nature of specific atmospheric scenarios, several studies have focused on FSO experiments conducted within controlled environment chambers. For example, an FSO link performance in desert environment was examined by simulating a dusty channel within a chamber [3]. The impact of indoor turbulence is analyzed by using a fan in [4]. However, these experiments lack practicality in their analyses due to their controlled chambers.

In this paper, we have established an FSO testbed at Korea University in Seoul with a total link distance of 400 m. To address the challenges of manually manipulating outdoor test environments, we automated the measurements to ensure frequent data collection. We measured bit-error rate (BER) at hourly intervals, allocating 4 minutes for each measurement. The data collection spanned from June $5^{th}$ to August $17^{th}$, yielding a total of 700 data sets. Corresponding atmospheric data were collected simultaneously. An analysis was conducted to examine how time and atmospheric condition affect FSO performance.

## II. FSO Atmospheric Turbulence Model

The classification of weak and strong turbulence ($h_s$) regimes is typically determined based on the magnitude of Rytov variance, denoted by $\sigma_R^2$ (or $\sigma_I^2$) [5]. The Rytov variance can be calculated by the following equation.

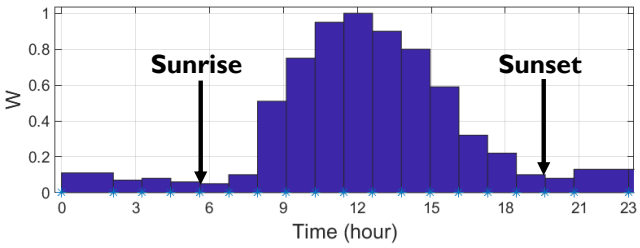


Fig. 1. Temporal Hour Weight with Sunrise at 5:37 and Sunset at 19:39

$$\sigma_R^2 = 1.23 C_n^2 k^{7/6} d^{11/6} \tag{1}$$

In (1), $k = 2\pi/\lambda$ means optical wave number ($\lambda$: wavelength) and $d$ indicate the propagation distance. $C_n^2$ means refractive-index structure parameter, which is expressed by BKB (Bendersky, Kopeika and Blaustein) model as follows [6]

$$\begin{aligned} C_n^2 &= 3.8 \cdot 10^{-14} W + 2 \cdot 10^{-15} T - 5.3 \cdot 10^{-13} \\ &- 2.8 \cdot 10^{-15} RH + 2.9 \cdot 10^{-17} RH^2 - 1.1 \cdot 10^{-19} RH^3 \\ &- 2.5 \cdot 10^{-15} W_s + 1.2 \cdot 10^{-15} W_s^2 - 8.5 \cdot 10^{-17} W_s^3 \end{aligned} \tag{2}$$

where $W$ is temporal hour weight, $T$ is the air temperature (in K), $RH$ is relative humidity (in %), and $W_s$ is wind speed (in m/s). A temporal hour is 1/12 of the time between sunrise and sunset. Fig. 1 shows an example of temporal hour weight when the sun rises at 5:37 AM and sets at 7:39 PM. This model is known for its high accuracy within the range of 282 to 308 K, relative humidity from 14 to 92%, and wind speed of up to 10 m/s.

In the weak atmospheric turbulence regime ($\sigma_R^2 \leq 0.3$), $h_s$ is known to follow log-normal distribution and its probability density function (PDF) is given by [1]

$$f_h(h_s) = \frac{1}{h_s \sqrt{2\pi\sigma_R^2}} \exp\left(-\frac{(\ln(h_s) + \frac{1}{2}\sigma_R^2)^2}{2\sigma_R^2}\right) \tag{3}$$

In the strong atmospheric turbulence regime ($\sigma_R^2 > 0.3$), $h_s$ is known to follow gamma-gamma function, which is given as

$$f_h(h_s) = \frac{2(\alpha\beta)^{(\alpha+\beta)/2}}{\Gamma(\alpha)\Gamma(\beta)} h_s^{\frac{\alpha+\beta}{2}-1} K_{\alpha-\beta}(2\sqrt{\alpha\beta h_s}) \tag{4}$$

where $K_n(\cdot)$ is the modified Bessel function of the $2^{nd}$ kind of order $n$ and $\Gamma(\cdot)$ denote the gamma function. $\alpha$ and $\beta$, respectively, denote the effective number of large- and small-scale eddies of the scattering process. Two parameters are given as the following equations.

$$\alpha = [\exp(\frac{0.49\sigma_R^2}{(1+1.11\sigma_R^{\frac{12}{5}})^{\frac{7}{6}}}) - 1]^{-1} \quad (5)$$

$$\beta = [\exp(\frac{0.51\sigma_R^2}{(1+0.69\sigma_R^{\frac{12}{5}})^{\frac{5}{6}}}) - 1]^{-1} \quad (6)$$

## III. Experiment Setup for Outdoor FSO

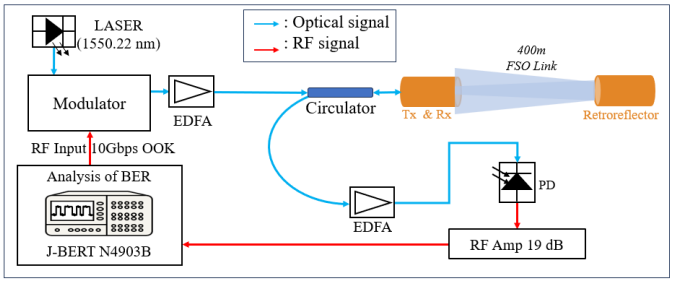


Fig. 2. Block Diagram of the Experiment Setup

Fig. 2 illustrates the block diagram of our experimental setup. The system comprises components distributed across a 400 m distance, including a laser source, EDFA (Erbium Doped Fiber Amplifier), SMF (single-mode fiber) cables, BERT (Bit Error Rate Tester), and other optical components. A 1,550 nm wavelength laser is modulated by an RF signal generated by BERT and the resulting signal is transmitted via a collimator. The optical signal travels 200 m to reach the retro-reflector, which reflects the signal back to Rx. The received signal passes through a circulator (Thorlabs 6015-3-APC) and goes to the PD (Photo-Detector) for conversion into an electrical signal. Subsequently, BERT measures BER for approximately 4 minutes during every measurement to enhance the measurement accuracy. We implement a simple automation app to enable BERT to measure BER automatically, transmitting about $2 \times 10^{12}$ bits hourly. The weather conditions at that time are collected together, including temperature, humidity, and wind speed. The atmospheric data is obtained from the government meteorological station that is closest to the laboratory. Additionally, we record sunrise and sunset times to calculate $W$, required for $C_n^2$ using (2). Fig. 3 provides a photograph of our outdoor FSO experiments in detail. Through this setup, we can conduct a 400 m FSO experiment using only a 200 m distance, while keeping both the Rx and Tx together. Since all of the equipment, except the retro-reflector, is indoor, the experiment can be conducted regardless of external weather conditions.

## IV. Result Analysis

### A. Analysis of the Impact of Sunlight : BER and $C_n^2$ over Time

Fig. 4 (a) shows $C_n^2$ from the collected atmospheric data over time along with a curve fitting graph utilizing a polynomial of a $4^{th}$ order. Notably, since $C_n^2$ is proportional to $W$, the calculated value of $C_n^2$ shows similar pattern of $W$ as in Fig. 1. This signifies a strong correlation between $C_n^2$ and $W$.

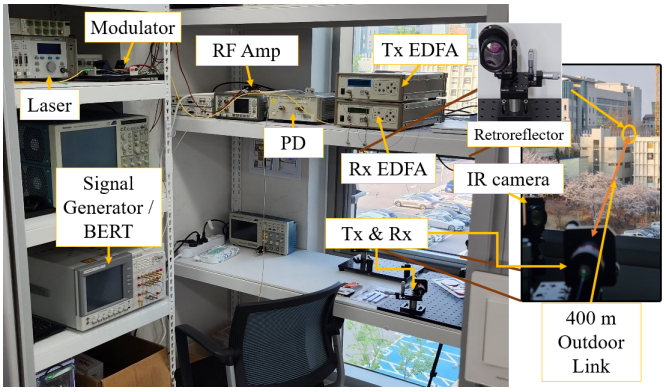


Fig. 3. Experiment Setup for a 400 m Outdoor FSO System

Fig. 4 (b) illustrates the time-dependent behavior of BER, accompanied by a corresponding curve fitting. As in (3) and (4), the PDF of atmospheric turbulence is affected by $C_n^2$. Consequently, the similarity in patterns observed between Fig. 4 (a) and (b) arises. This indicates that atmospheric turbulence is strongly affected by sun light.

The green dotted line in Fig. 4 (b) represents the forward error correction (FEC) limit ($= 3.8 \cdot 10^{-3}$) [7]. Instances of outage conditions surpassing this limit accounted for about 11% of the total measurements. Most of the outage condition occurred between sunrise time (6:00 AM), and sunset time (8:00 PM). As $W$ increases during daylight hours, subsequently leading to an elevation in $\sigma_R^2$, the BER performance experiences a decline during daylight periods. Through the accumulation of a substantial dataset ensuring high reliability, experimental findings have verified that sunlight influences communication performance in comparison to other meteorological factors.

### B. Comparison of BER Performance between Rainy and Non-Rainy Conditions

Fig. 5 illustrates BER performance over time in rainy and non-rainy conditions, accompanied by corresponding curve fittings. The curve fitting for rainy days reveals consistent BER performance distribution due to reduced sunlight influence. This outcome can be attributed to the declined influence of sunlight on rainy days. Conversely, non-rainy days exhibit same pattern to Fig. 4 (b), supporting sunlight's impact on FSO communication performance. Rainy days saw 20% outages, whereas non-rainy days only had 10%. Among the outages on rainy days, approximately 1/3 occurred during periods of heavy rainfall, including the time interval from 2:00 AM to 4:00 AM, which typically exhibits better performance on non-rainy days. This underscores rainfall's effect on communication performance.

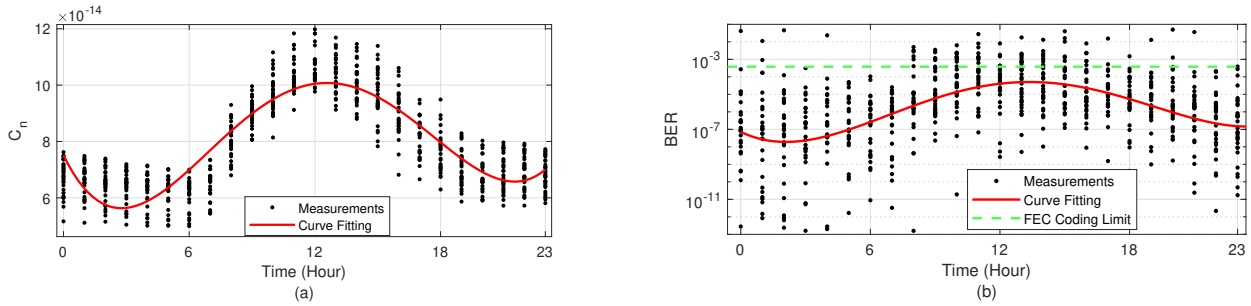


Fig. 4. Experimental Results for (a) $C_n^2$ (b) BER over Time

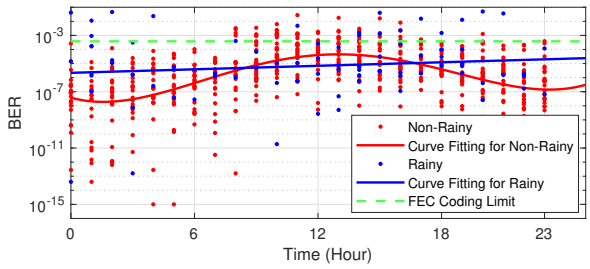


Fig. 5. Experimental Results for BER over Time on Rainy and Non-Rainy Days

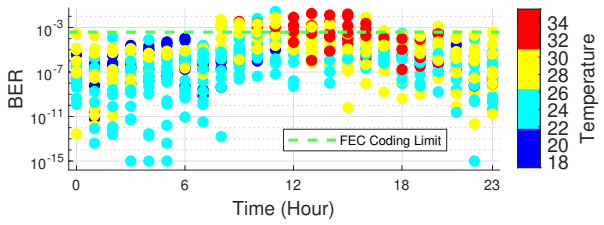


Fig. 6. Experimental Results for BER over Time and Temperature

### C. Comparison of BER Performance over Time and Temperature

Fig. 6 displays a scatter plot correlating BER with temperature on non-rainy days. Cooler colors signify lower temperatures, while warmer colors indicate higher temperatures. Comparing performance at the same times reveals better results with lower temperatures. Most data points within the lower temperature range are below the FEC limit, but some in higher temperatures approach or exceed it. As temperature rises, following (2), $C_n^2$ increases, negatively affecting communication. Despite the absence of temperatures below 18°C, since the observation is done from June to August, this underscores temperature's impact on FSO communication.

Throughout the results above, the experimental evidence confirms that FSO communication performance is influenced by sunlight, temperature, and rainfall. Remarkably, the FSO performance is observed to be better in less sunlight, lower temperatures, and lower rainfall. Importantly, our experiments were conducted outdoors, rather than within a controlled chamber, offering practical data collection. Since all equipment is indoors and automatically operates, the experiments could be conducted frequently regardless of weather conditions

## V. Conclusion

In this paper, we delved into performance analysis of an outdoor 400 m FSO communication system during the summer season. The experimental results establish that the communication performance is improved during the time without sunlight. The influential role of temperature and rainfall on FSO performance is also confirmed. We obtained reliable data by conducting experiments in a real-world outdoor setting rather than indoor chamber and adopting automated measurement. For future works, if data for other seasons are collected later, it seems feasible to develop a new FSO channel model based on Korean meteorological conditions.


## Acknowledgment

This work was supported by Institute of Information & communications Technology Planning & Evaluation (IITP) grant funded by the Korea government(MSIT) (2021-0-00260, Research on LEO Inter-Satellite Links)


## References


[1] Z. Ghassemlooy, W. Popoola, and S. Rajbhandari, *Optical Wireless Communications: System and Channel Modelling with MATLAB*. Boca Raton, FL: Taylor & Francis, 2013.

[2] J. C. Ricklin, S. M. Hammel, F. D. Eaton, and S. L. Lachinova, "Atmospheric channel effects on free-space laser communication," *Journal of Optical and Fiber Communications Reports*, vol. 3, no. 2, pp. 111–158, Apr. 2006.

[3] M. A. Esmail, H. Fathallah, and M.-S. Alouini, "An Experimental Study of FSO Link Performance in Desert Environment," *IEEE Communications Letters*, vol. 20, no. 9, pp. 1888–1891, Sep. 2016.

[4] J. L. Nascimento, M. A. Fernandes, F. P. Guiomar, and P. P. Monteiro, "Experimental Analysis of the Impact of Indoor Turbulence on FSO for Intra-Datacenter Communications," in *2021 Telecoms Conference (ConfTELE)*, Feb. 2021, pp. 1–5.

[5] A. K. Majumdar, *Advanced Free Space Optics (FSO): A Systems Approach*, ser. Springer Series in Optical Sciences. New York, NY: Springer New York, 2015, vol. 186.

[6] S. Bendersky, N. S. Kopeika, and N. Blaunstein, "Atmospheric optical turbulence over land in middle east coastal environments: Prediction modeling and measurements," *Applied optics*, vol. 43, no. 20, pp. 4070–4079, 2004.

[7] M. A. Esmail, A. Ragheb, H. Fathallah, and M.-S. Alouini, "Investigation and Demonstration of High Speed Full-Optical Hybrid FSO/Fiber Communication System Under Light Sand Storm Condition," *IEEE Photonics Journal*, vol. 9, no. 1, pp. 1–12, Feb. 2017.